Federal Aviation Administration

DOT/FAA/AM-10/5
Office of Aerospace Medicine
Washington, DC 20591

Evaluation of the Effects of Hydrogen Peroxide on Common Aircraft Electrical Materials

Sin Ming Loo, Josh Kiepert, Derek Klein, Michael Pook
Boise State University
Boise, ID 83725

Shih-Feng Chou, Tony Overfelt
Auburn University
Auburn, AL 36849

Jean Watson
Office of Aerospace Medicine
Federal Aviation Administration
Washington, DC 20591

March 2010

Final Report

OK-10-0077-JAH

NOTICE

Technical Report Documentation Page

1. Report No.	2. Government Accession No.	3. Recipient's Catalog No.
DOT/FAA/AM-10/5		

4. Title and Subtitle	5. Report Date
Evaluation of the Effects of Hydrogen Peroxide on Common Aircraft Electrical Materials	March 2010
	6. Performing Organization Code

7. Author(s)	8. Performing Organization Report No.
Loo SM,[1] Kiepert J,[1] Klein D,[1] Pook M,[1] Chou SF,[2] Overfelt T,[2] Watson J[3]	

9. Performing Organization Name and Address	10. Work Unit No. (TRAIS)
[1]National Air Transportation Center of Excellence for Research in the Intermodal Transport Environment Boise State University, Boise, ID 83725 [2]National Air Transportation Center of Excellence for Research in the Intermodal Transport Environment Auburn University, Auburn AL 36849 [3]Office of Aerospace Medicine Federal Aviation Administration Washington, DC 20591	11. Contract or Grant No. Co-Op Agrmt No. 07-C-RITE-BSU

12. Sponsoring Agency name and Address	13. Type of Report and Period Covered
Office of Aerospace Medicine Federal Aviation Administration 800 Independence Ave., S.W. Washington, DC 20591	14. Sponsoring Agency Code

15. Supplemental Notes
Work was accomplished under Public law 108-76

16. Abstract
Aircraft can be contaminated with unwanted chemical or biological elements. For years, hydrogen peroxide has been used to disinfect equipment in the medical community. The diluted vapor form of hydrogen peroxide is being considered for use as a decontaminant/disinfectant/sanitizer of transportation vehicles aircraft, buses, subway trains, ambulances, etc. Previous work showed that STERIS Corporation's Vaporized Hydrogen Peroxide (VHP®) technology could be used successfully in complex transportation vehicles. However, the compatibility of the process with typical aircraft avionics has not been established. This report documents a preliminary evaluation of the effects of hydrogen peroxide exposure on avionics (i.e., avionics wires, active circuit boards, and dummy circuit boards).

17. Key Words	18. Distribution Statement
Aircraft Avionics, Printed Circuit Board, VHP, High Voltage	Document is available to the public through the Defense Technical Information Center, Ft. Belvoir, VA 22060; and the National Technical Information Service, Springfield, VA 22161

19. Security Classif. (of this report)	20. Security Classif. (of this page)	21. No. of Pages	22. Price
Unclassified	Unclassified	18	

Form DOT F 1700.7 (8-72) Reproduction of completed page authorized

CONTENTS

ABBREVIATIONS

As used in this report, the following abbreviations/acronyms have the meanings indicated

Abbreviation	Meaning
BI	Biological Indicator
DSC	Differential Scanning Calorimetry
ppm	Parts Per Million
RMS	Root Mean Squared
VHP®	Vaporized Hydrogen Peroxide
XPS	X-ray Photoelectron Spectroscopy

Evaluation of the Effects of Hydrogen Peroxide on Common Aircraft Electrical Materials

INTRODUCTION

Among all of the large-scale disinfection and/or decontamination technologies available, vaporized hydrogen peroxide (VHP®)[1] is of particular interest due to its rapid sterilization, easy usage, intrinsic environmental friendliness (i.e. simple by-products composed of only water and oxygen), and compatibility with many materials and systems. VHP® technology has been investigated for possible usage in aircraft applications (1-4). These studies used vaporized hydrogen peroxide concentrations in the range of 150 - 600 ppm and cycle times of 80 - 120 min. Maximum concentrations of hydrogen peroxide vapor were carefully controlled to avoid condensation in cool locations within the aircraft cabins. Although these studies did not evaluate the compatibility of the various cabin materials with exposure to vaporized hydrogen peroxide, analysis of the collected data showed that VHP® did not seem to have any visible effect on the materials (3).

A typical VHP® process cycle consists of an initial dehumidification step, then a conditioning phase followed by the actual sanitization/ decontamination process. Finally, an aeration phase is employed to remove residual hydrogen peroxide vapor. During the dehumidification phase, warm, dry air flows into the enclosure to lower the relative humidity to less than 10%. This allows a higher concentration of hydrogen peroxide vapor to be injected into the enclosure without causing condensation. Hydrogen peroxide liquid concentrate (35% liquid H_2O_2 with a pH ~ 3) is then flash vaporized and injected into the enclosure during the initial conditioning and sanitization/decontamination phases. The purpose of the conditioning phase is to rapidly increase the hydrogen peroxide concentration to minimize the overall cycle time. During the sanitization/ decontamination phase, a steady concentration of hydrogen peroxide vapor (typically 250 - 450 ppm) is maintained. This produces the desired sanitization/decontamination effect that is often measured by the 6-log kill (i.e., 10^6 reduction) of a commercial biological indicator (BI) spore population of *Geobacillus stearothermophilus*. Once the sanitization/ decontamination phase is completed, the enclosure is aerated with fresh air while any residual hydrogen peroxide vapor breaks down into environmentally benign water and oxygen.

[1] VHP is a registered trademark of STERIS Corporation, Mentor, OH, USA.

Many polymeric materials are known to be susceptible to absorption of moisture. The small water molecules diffuse into the polymer matrix and force apart the polymer macromolecules, causing swelling. Increases in the distance between the polymer chains reduce the strength of the secondary intermolecular bonds and increase the softness and ductility of the polymer. However, the highly cross-linked epoxies used in aerospace-grade fiber composites minimize moisture absorption. Thus, these materials exhibit good resistance to degradation in wet environments (5). While molecules of H_2O_2 vapor should be absorbed even less by epoxies than H_2O molecules, the intermolecular cross-links might be degraded by oxidation from the hydrogen peroxide. The extensive usage of fiber/epoxy composites in aerospace structures and avionics dictates that the compatibility of these materials with hydrogen peroxide vapor be examined.

Although several similarities exist between the contents of this report and technical report entitled "Evaluation of the Effects of Hydrogen Peroxide on Common Aviation Structural Materials" (1), this document includes an analysis of VHP's effect on avionics materials not found in the other report.

METHODS AND MATERIALS

The specific motivation for this work was to evaluate the compatibility of avionic materials. At the early stage of the work, multiple attempts were made to obtain used aircraft avionic printed circuit boards to test the VHP® compatibility. The use of real aircraft avionic printed circuit boards was not pursued further due to the following reasons:

- History of the avionics: With used avionics, obtaining the operational history is difficult or impossible. Thus, it would be nearly impossible to set up control cases for comparison.
- Difficulty in obtaining the test equipment: Assuming avionics were obtainable, the test equipment required to analyze the avionics was determined either to be impossible to obtain or too expensive.

Given these challenges, the decision was made to design dummy and active printed circuit boards. The dummy circuit board had no active components. The active board had operational components including voltage level converters, a microcontroller, resistors, capacitors, and

connectors. In addition to these boards, avionics wires were also used as test samples (see Figure 1).

Test Setup for Dummy Circuit Board

In order to study different characteristics, tests were performed on several different dummy circuit board layouts, active board, and aviation wire. The three dummy board layouts were wire, interdigitated, and pad. The wire board layout shown in Figure 1(a) was used to test the effects of VHP® on the impedance of traces. The interdigitated board layout shown in Figure 1(b) was used to test how VHP® affected the impedance between traces. The pad board layout shown in Figure 1(c), was used to test the effects of VHP® on pad impedance. A board with active component (microcontroller) was designed to test the effect of VHP® (Figure 1(d)). Aviation wire was also used in our tests (Figure 1(e)). A HP4263B Inductance, Capacitance, and Resistance (LCR) meter (Figure 2) was used to measure the impedance of the traces on each board. For the wire boards, the impedances of all 16 traces were measured at 100mV, 1kHz. For the interdigitated boards, the impedances were measured at 100mV, 1kHz, and 10kHz. For the pad boards, the impedances were measured at 100mV, 1kHz. Figure 2 shows the test setup. The resistance of the wires was measured and subtracted from the trace measurements to obtain the impedance of the traces themselves.

Results from the research indicated that a conformal coating is normally applied to avionics circuit boards. Therefore, some of the samples were coated with 1B31 acrylic coating (HumiSeal Protective Coatings; Woodside, NY.) Multiple tests were performed for each board layout (uncoated, uncoated-VHP® exposed, conformal coated, and conformal coated-VHP® exposed).

Test Setup for Active Circuit Board

To test the active boards, sine and square waves were generated by the active boards to verify the signal output capabilities. As the active circuit was digital in nature, the square wave output could be directly generated. The sine wave signal was generated through pulsewidth-modulation and a filter circuit. The signals for the unexposed boards and the VHP® exposed boards were recorded and compared by using an oscilloscope. Figure 3 shows the testing circuit for sine wave and square wave acquisition from the active board.

For input acquisition tests on the active boards, a function generator was configured to output a sine

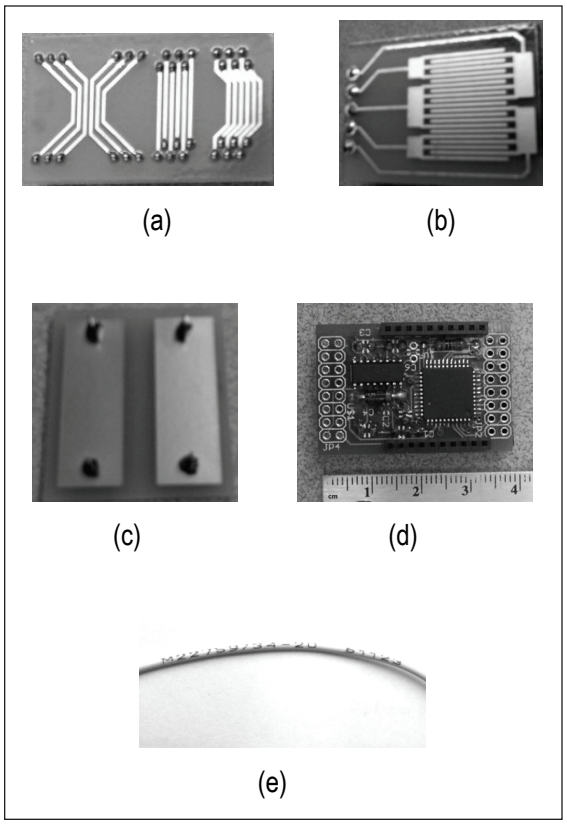

Figure 1: Wire Board (Fig. a), Interdigitated Board (Fig. b) [6], Pad Board (Fig. c), Active Board (Fig. d), and Aviation (MILSPEC) Wire (Fig. e)

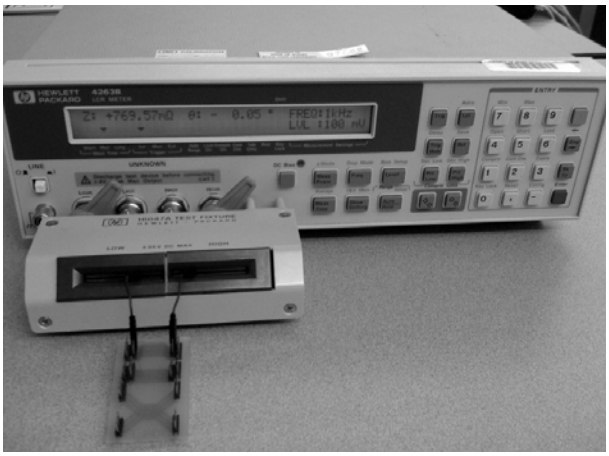

Figure 2: Test Setup for Dummy Boards

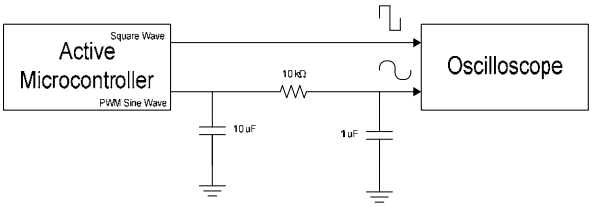

Figure 3: Active Circuit Output Configuration

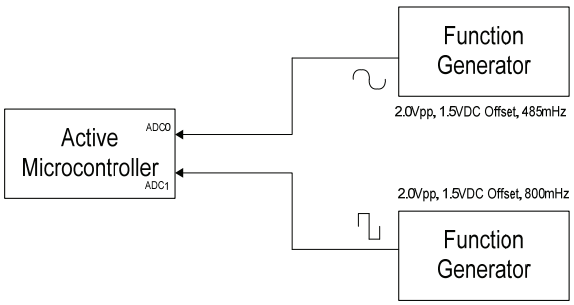

Figure 4: Active Circuit Input Configuration

wave or square wave, which would be captured with the analog-to-digital converter present in the active circuit board (microcontroller). Figure 4 shows the circuit used.

Test Setup for Wires

To test for any potential degradation of the aviation wire insulation (MIL227597/34-20), a high-voltage power supply and current measuring electronics were set up to apply high-voltage stress to the insulation (Figure 5). This was done in to determine the effect of VHP® exposure

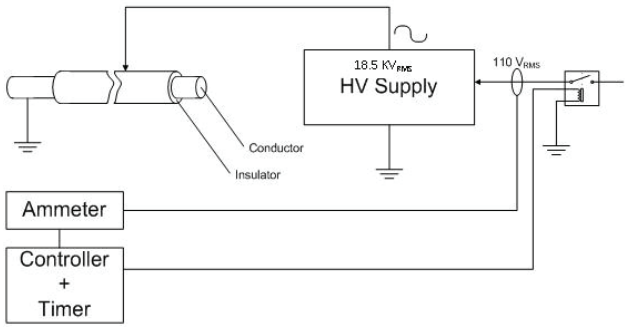

Figure 5: VHP Wire Insulation Stress Configuration

on the time-to-breakdown of the wire insulation. In this set of tests, ~18.5 KV RMS at 60 Hz was applied to ~1 ft sections of aviation wire. One terminal was connected to one end of the wire with the insulation intact. The other terminal was connected to the wire's conductor. The high-voltage power supply system kept a record of when the insulation breakdown occurred (VHP®- exposed wires versus non-VHP® exposed wires). Twenty samples were tested for both exposed and non-exposed wires. Breakdown was detected by the current spike associated with the resulting short circuit.

VHP® Decontamination Processes

The printed circuit board and aviation wire specimens were subjected to 25 VHP® cycles and 10 VHP® cycles of decontamination processes, respectively. The cycles were designed to increase the aggressiveness of the decontamination environment where the chamber concentration was maintained at 450 ppm, and the inlet concentration was ~ 2000 ppm. Each cycle lasted for a total of 6.5 hrs, and the decontamination phase was held to 4.5 hrs. During the exposure of vaporized hydrogen peroxide, the printed circuit boards were placed on a stainless steel rack with the circuits facing upward to achieve the maximum contact to the vapor. The aviation wire samples were detached from a coil form and stretched out randomly inside the VHP® chamber to avoid surface contact between materials, which provided maximum exposure to the vapor.

RESULTS AND DISCUSSION

Test Results for Dummy Circuit Boards

In this study, each of the Dummy circuit board layouts was divided into two categories: conformal coated and non-coated. Within each category, only half of the samples were exposed to VHP®.

Wire Board Results

The average resistance of the long, medium, and short length traces was about 11, 8, and 7 MOhms, respectively (Figure 6 and Tables 1 to 4). The results had a small standard deviation across all measurements less than 0.01 MOhms. From the measurements, the longer traces had slightly more resistance than the shorter ones, but there was only about a 1 MOhm difference between the non-exposed versus exposed boards. This difference is so small that it would not affect the DC characteristics of the traces.

Interdigitated Board Results

The impedance between the traces was measured on the interdigitated board. Since the traces were unconnected, they behaved like a capacitor with air as the dielectric. As a result, the magnitude of the impedance measured was large (in the MOhm range), and the standard deviation was also large (on the order of 100-500 kOhms) (Tables 5 to 8, Figures 7 to 10). The plots in the figures above clearly show that the impedance does change on the order

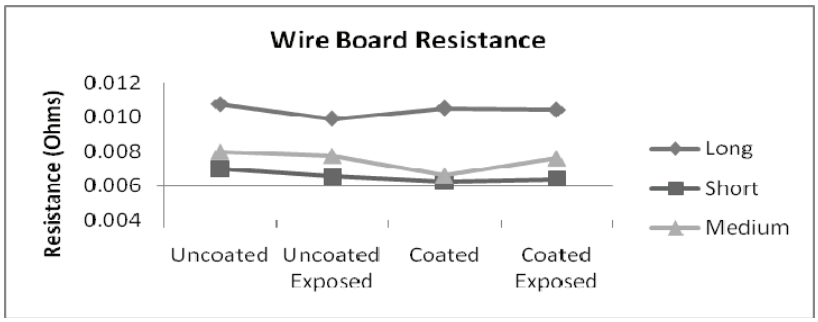

Figure 6: Wire Board Trace Resistance Summary

Table 1: Uncoated & Unexposed Impedance

Uncoated		
	Avg	Stdev
Long Mag (Ohms)	0.011	0.0015
Long Phase (Deg)	0.008	0.0041
Short Mag (Ohms)	0.007	0.0011
Short Phase (Deg)	0	0.0018
Med Mag (Ohms)	0.008	0.0017
Med Phase (Deg)	0.004	0.005

Table 2: Uncoated & Exposed Impedance

Uncoated-Exposed		
	Avg	**Stdev**
Long Mag (Ohms)	0.01	0.0044
Long Phase (Deg)	0.008	0.0041
Short Mag (Ohms)	0.007	0.0013
Short Phase (Deg)	0.002	0.0038
Med Mag (Ohms)	0.008	0.0019
Med Phase (Deg)	0.005	0.0051

Table 3: Coated & Unexposed Impedance

Coated		
	Avg	**Stdev**
Long Mag (Ohms)	0.01	0.0017
Long Phase (Deg)	0.008	0.0038
Short Mag (Ohms)	0.006	0.0014
Short Phase (Deg)	0.001	0.0035
Med Mag (Ohms)	0.007	0.0015
Med Phase (Deg)	0.004	0.005

Table 4: Coated & Exposed Impedance

Coated-Exposed		
	Avg	**Stdev**
Long Mag (Ohms)	0.01	0.0019
Long Phase (Deg)	0.009	0.0055
Short Mag (Ohms)	0.006	0.0012
Short Phase (Deg)	0.001	0.0031
Med Mag (Ohms)	0.008	0.0017
Med Phase (Deg)	0.003	0.0053

Table 5: Interdigitated Uncoated-Unexposed Impedance

Frequency	1KHz					10KHz			
Traces	1 & 2	1 & 3	3 & 5	4 & 5		1 & 2	1 & 3	3 & 5	4 & 5
Mag Avg	3.75E+07	4.23E+07	4.18E+07	3.73E+07		3.77E+06	4.22E+06	4.28E+06	3.80E+06
Mag StdDev	4.67E+05	5.85E+05	2.45E+05	4.93E+05		2.65E+04	3.44E+04	3.32E+04	4.51E+04
Phs Avg	-89.35	-89.24	-89.49	-89.04		-89.46	-89.44	-89.48	-89.44
Phase StdDev	0.26	0.47	0.33	0.37		0.09	0.05	0.04	0.05

Table 6: Interdigitated Uncoated-Exposed Impedance

Frequency	1KHz					10KHz			
Traces	1 & 2	1 & 3	3 & 5	4 & 5		1 & 2	1 & 3	3 & 5	4 & 5
Mag Avg	3.80E+07	4.28E+07	4.21E+07	3.79E+07		3.79E+06	4.21E+06	4.32E+06	3.83E+06
Mag StdDev	2.95E+05	3.83E+05	9.11E+05	4.85E+05		3.21E+04	5.77E+04	3.63E+04	3.74E+04
Phs Avg	-89.82	-89.76	-89.74	-89.9		-89.58	-89.52	-89.6	-89.56
Phase StdDev	0.08	0.17	0.11	0.07		0.04	0.04	0	0.05

Table 7: Interdigitated Coated-Unexposed Impedance

Frequency	1KHz					10KHz		
Traces	1 & 2	1 & 3	3 & 5	4 & 5	1 & 2	1 & 3	3 & 5	4 & 5
Mag Avg	3.66E+07	4.11E+07	4.02E+07	3.62E+07	3.65E+06	4.04E+06	4.14E+06	3.68E+06
Mag StdDev	3.44E+05	1.92E+05	1.95E+05	3.70E+05	4.83E+04	5.50E+04	2.17E+04	1.64E+04
Phs Avg	-89.7	-89.76	-89.66	-89.76	-89.5	-89.5	-89.5	-89.5
Phase StdDev	0	0.09	0.13	0.13	0	0	0	0

Table 8: Interdigitated Coated-Exposed Impedance

Frequency	1KHz					10KHz		
Traces	1 & 2	1 & 3	3 & 5	4 & 5	1 & 2	1 & 3	3 & 5	4 & 5
Mag Avg	3.68E+07	4.15E+07	4.10E+07	3.65E+07	3.67E+06	4.08E+06	4.16E+06	3.70E+06
Mag StdDev	3.08E+05	4.93E+05	4.88E+05	3.58E+05	3.11E+04	7.05E+04	5.15E+04	2.55E+04
Phs Avg	-89.72	-89.7	-89.78	-89.76	-89.5	-89.5	-89.5	-89.5
Phase StdDev	0.04	0.14	0.18	0.13	0	0	0	0

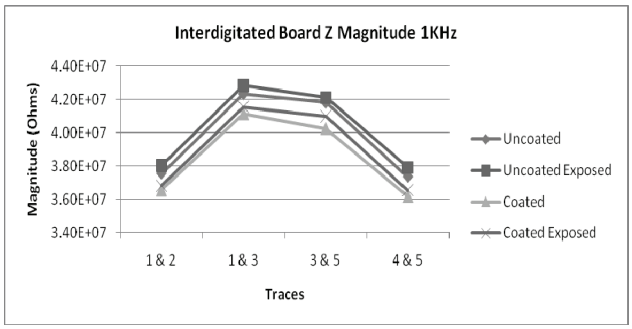

Figure 7: Interdigitated Z Magnitude, 1KHz

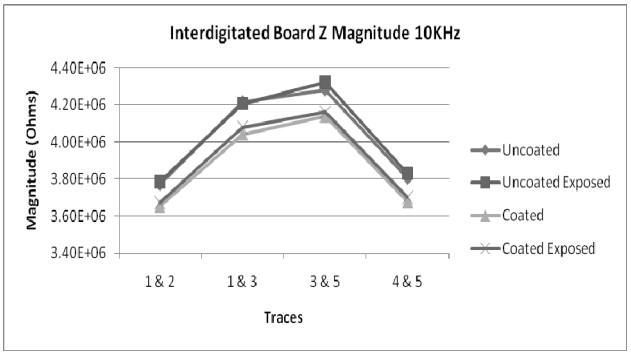

Figure 8: Interdigitated Z Magnitude, 1KHz

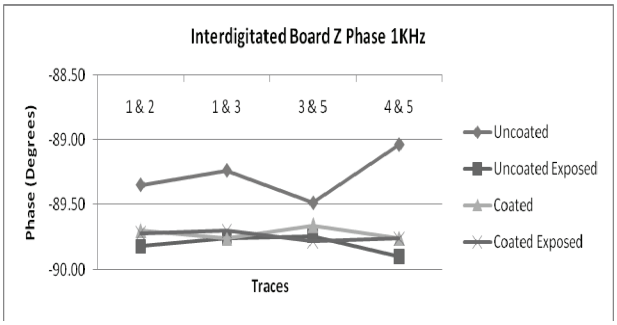

Figure 9: Interdigitated Z Phase, 1KHz

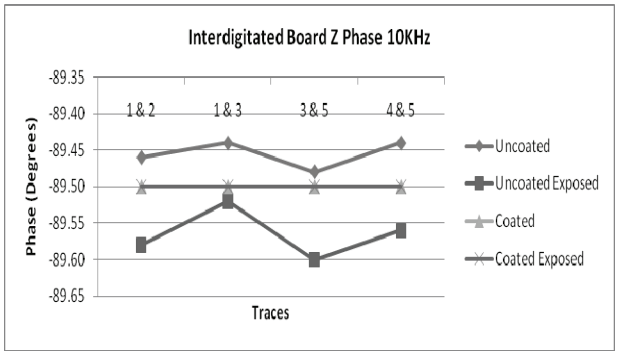

Figure 10: Interdigitated Z Phase, 10KHz

Table 9: Pad Boards Impedance Results

Uncoated			Uncoated-Exposed		
	Avg	Stdev		Avg	Stdev
Mag (Ohms)	0.764	0.002	Mag (Ohms)	0.762	0.001
Phase (Deg)	-0.08	0	Phase (Deg)	-0.081	0.003
Coated			**Coated-Exposed**		
	Avg	Stdev		Avg	Stdev
Mag (Ohms)	0.763	0.002	Mag (Ohms)	0.763	0.001
Phase (Deg)	-0.08	0	Phase (Deg)	-0.08	0

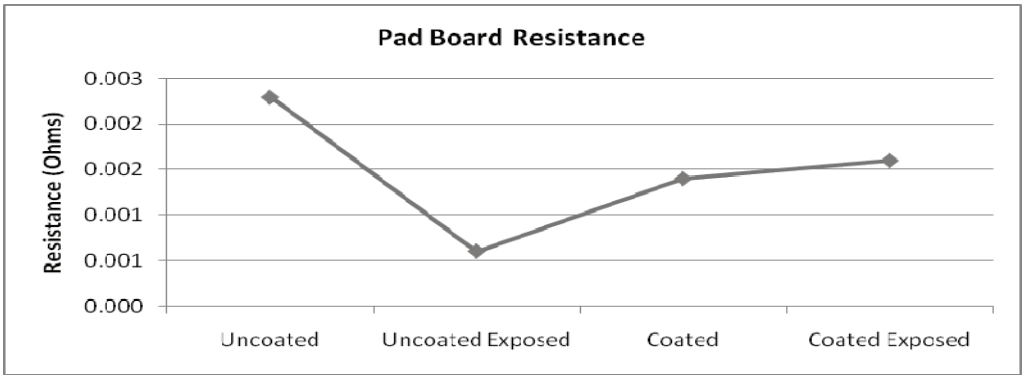

Figure 11: Pad Board Resistance Summary

of about 2 MOhms with respect to the various coatings and exposures. The largest change was between the coated and uncoated-exposed boards, which had a 1.46 MOhm difference. This was most likely caused by the coating affecting the capacitance of the traces. Compared to the standard deviation of about 0.5 kOhms, this difference is insignificant to the performance of the traces. At 10kHz, a similar trend, followed with the values being scaled down by a factor of 10. The phase between the traces had small changes that were insignificant with respect to their performance.

Pad Board Results

The pad board resistance had a maximum difference of approximately 2 MOhms between the uncoated and uncoated-exposed boards (Table 9 and Figure 11). Since the standard deviation was about 1 MOhm, this change was insignificant.

In summary, the results indicated that there were no statistical differences between the boards that were exposed to VHP® and those that were not exposed. These tests were carried out on boards without solder mask. Solder mask (as is found on a typical PCB) would have provided another layer of protection against corrosion. The Auburn team found that a very thin layer of copper oxidation was present on the tested boards. However, some oxidation due to air exposure would have occurred on these unprotected boards even without the presence of VHP®.

Test Results for Active Board

As is clear from the figures (Figures 12 to 27), the pre-and post-generated/measured waveforms were found to match with only minor deviations that may be attributed to expected noise. The input and output signals of unexposed boards and VHP® exposed boards were compared. No statistical difference was found, and the ability of the active boards to output or acquire signals was not found to be diminished in any way by the exposure to VHP®. However, oxidation was visible on unprotected tin contacts.

Test Results of Aviation Wires

Figure 28 shows the results. Wires not exposed to VHP® failed within 16 minutes on average. The wires that were exposed to VHP® failed on average within 4 minutes. This indicates that VHP® did change the dielectric strength of the wire insulation. However, in the interest of increasing the speed at which the breakdown would occur, the voltage stress applied was outside the operational voltages experienced by aviation wire. The

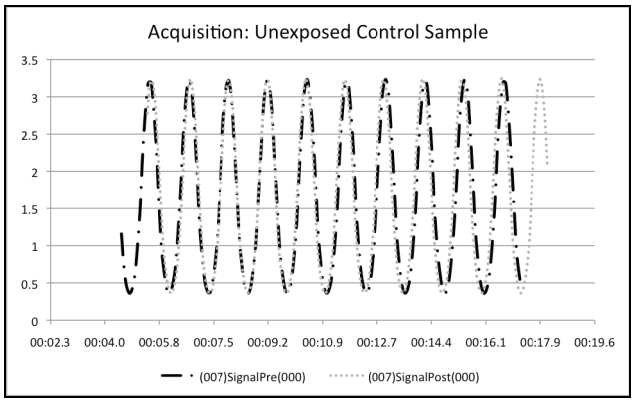

Figure 12: 01 - Acquisition Sine Wave, 485mHz, 2.0Vpp, 1.5V DC offset (unexposed)

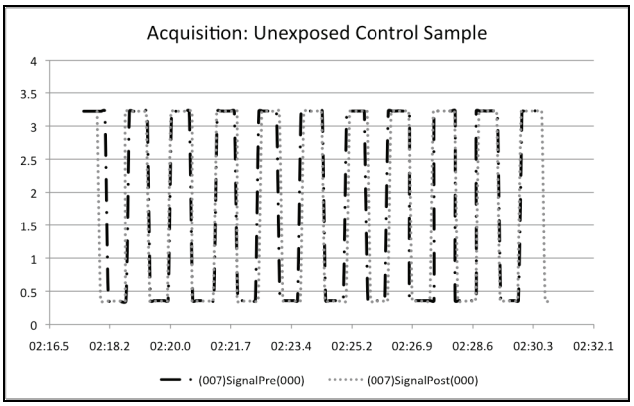

Figure13: 01 - Acquisition Square Wave, 485mHz, 2.0Vpp, 1.5V DC offset (unexposed)

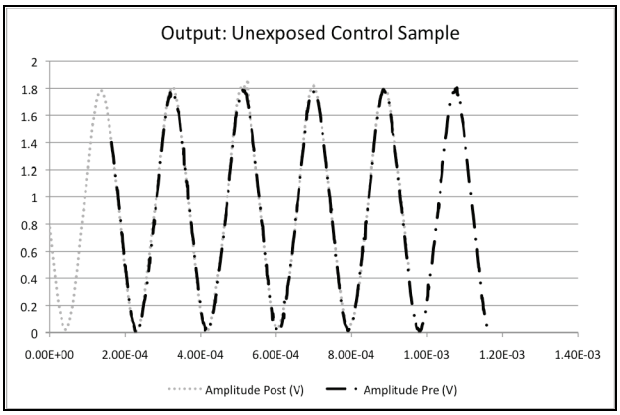

Figure 14: 01 - Output Sine Wave (Unexposed)

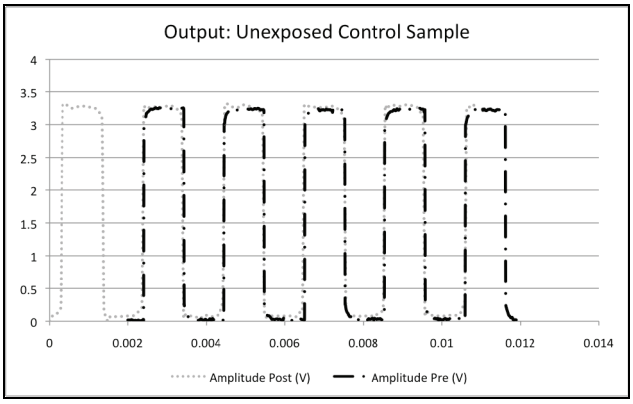

Figure 15: 01 - Output Square Wave (Unexposed)

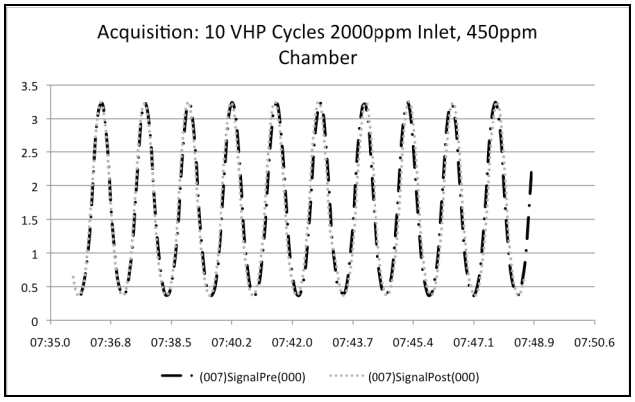

Figure16: 02 - Acquisition Sine Wave, 485mHz, 2.0Vpp, 1.5V DC Offset (10@2000ppm)

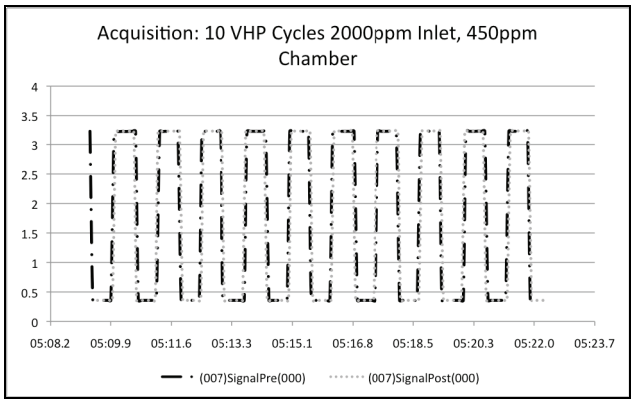

Figure 17: 02 - Acquisition Square Wave, 485mHz, 2.0Vpp, 1.5V DC offset (10@2000ppm)

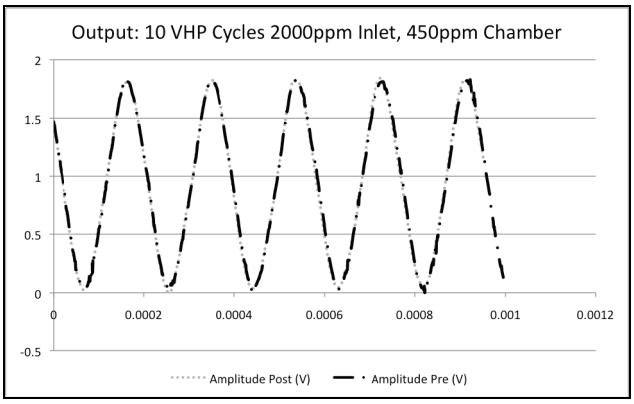

Figure 18: 02 - Output Sine Wave (10@2000ppm)

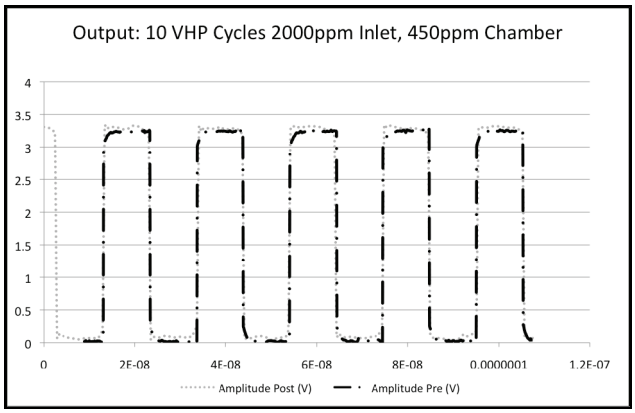

Figure 19: 02 - Output Square Wave (10@2000ppm)

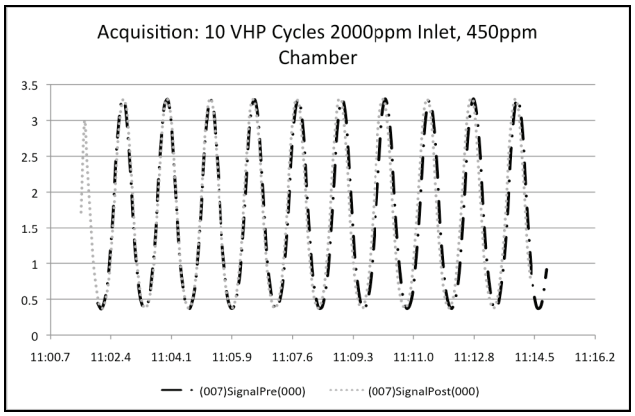

Figure 20: 03 - Acquisition Sine Wave, 485mHz, 2.0Vpp, 1.5V DC offset (10@2000ppm)

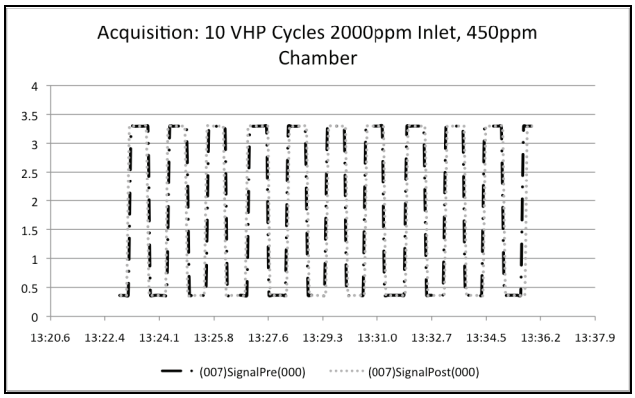

Figure 21: 03 - Acquisition Square Wave, 485mHz, 2.0Vpp, 1.5V DC offset (10@2000ppm)

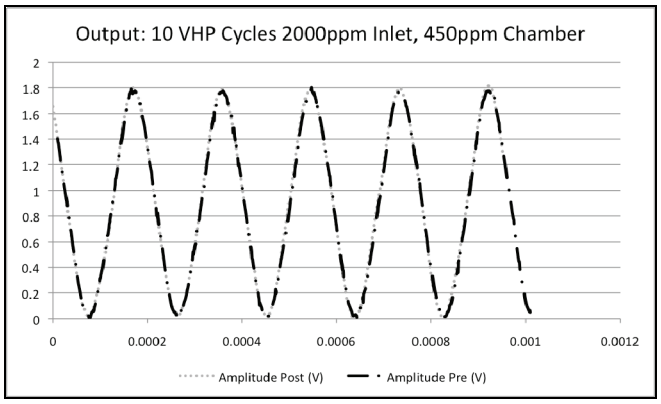

Figure 22: 03 - Output Sine Wave (10@2000ppm)

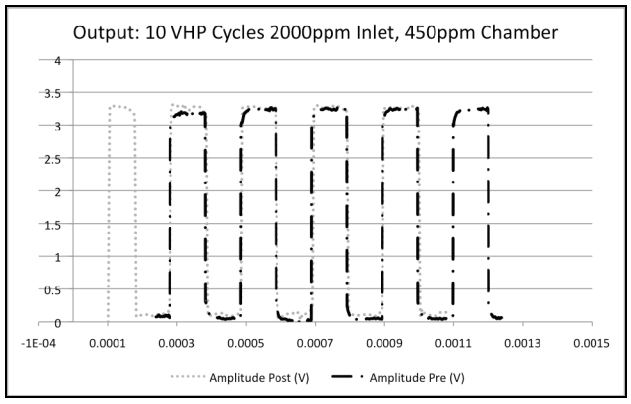

Figure 23: 03 - Output Square Wave (10@2000ppm)

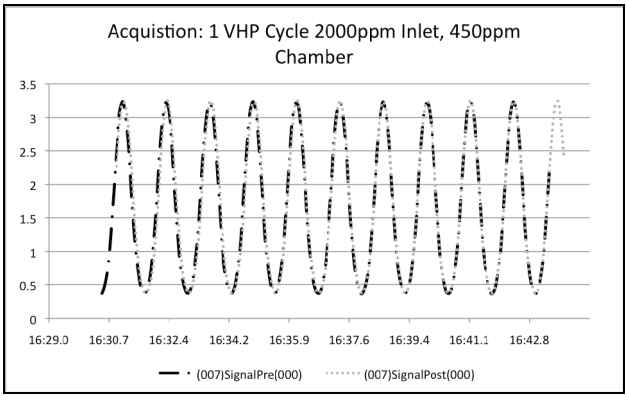

Figure 24: 04 - Acquisition Sine Wave, 485mHz, 2.0Vpp, 1.5V DC offset (1@2000ppm)

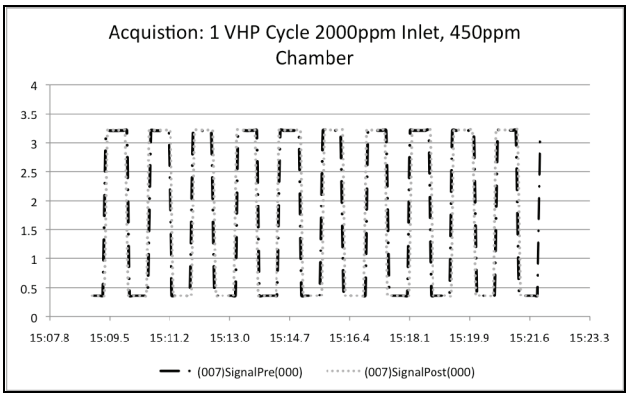

Figure 25: 04 - Acquisition Square wave, 485mHz, 2.0Vpp, 1.5V DC offset (1@2000ppm)

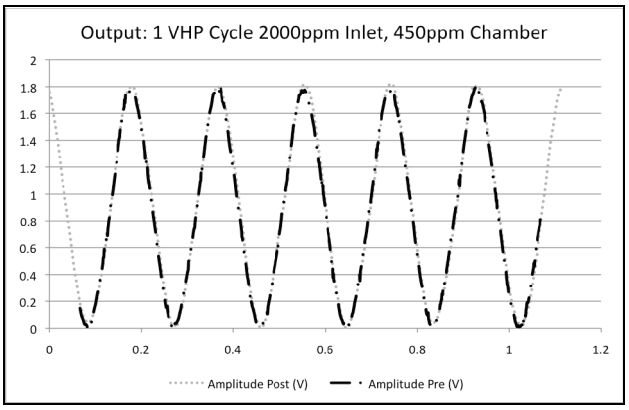

Figure 26: 04 - Output Sine Wave (1@2000ppm)

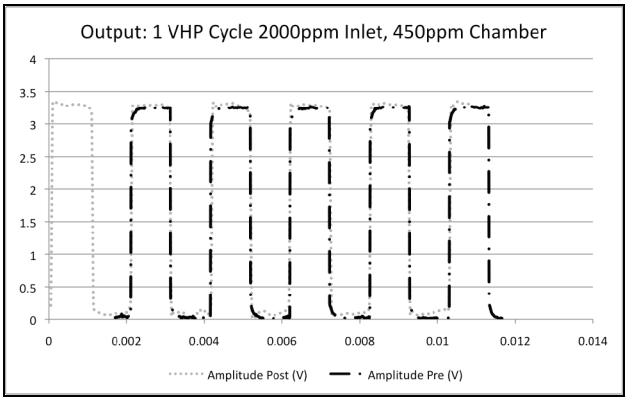

Figure 27: 04 - Output Square Wave (1@2000ppm)

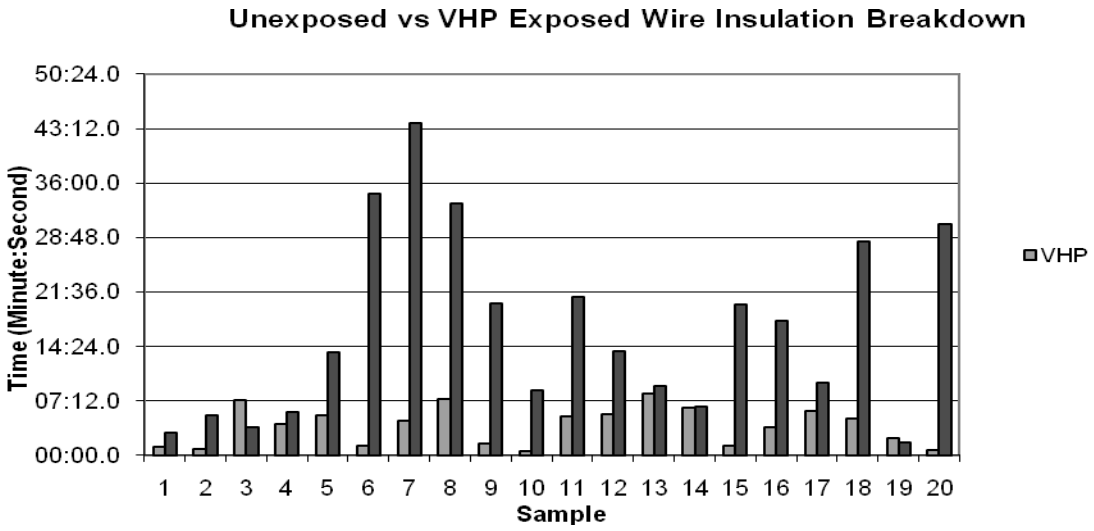

Figure 28: Results of Pre-VHP® and Post-VHP® Aviation Wire Tests

Table 10: Percentage Weight Change of the Print Circuit Boards and Aviation Wire After VHP® Treatment

Specimen	Percentage Weight Change (Standard Deviation), %						
	Uncoated			Coated			Aviation
	Pad	Wire	Interdigitated	Pad	Wire	Interdigitated	Wire
	-0.04 (0.01)	-0.06 (0.01)	-0.07 (0.01)	-0.03 (0.01)	-0.05 (0.02)	-0.07 (0.01)	0.07 (0.01)

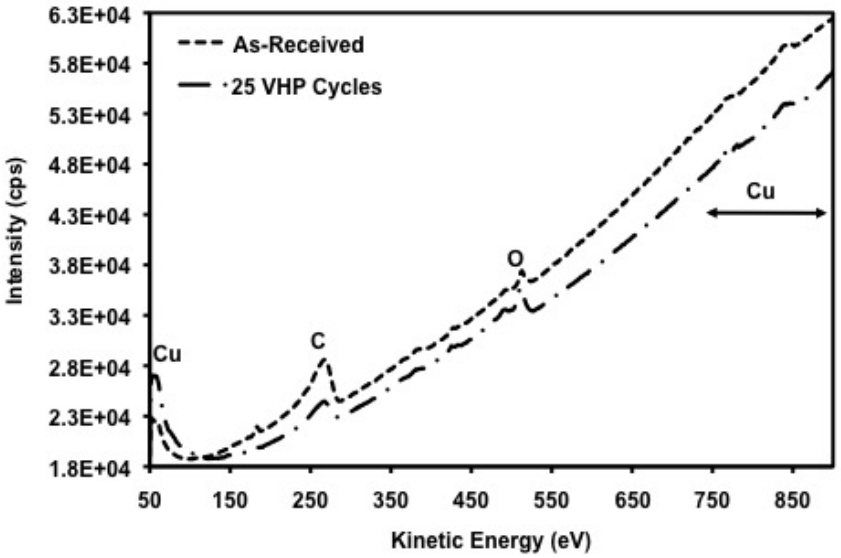

Figure 29: Auger Electron Spectroscopy of Copper on the Print Circuit Boards

stress voltage was ~18.5 KV_{RMS} for these tests, whereas the normal aircraft operating voltage is 28 Volts at 400 Hz. The next set of tests will be carried out at voltages closer to the operational range.

Weight Change of Printed Circuit Boards and Wires

Weight change on the specimens due to the exposure of hydrogen peroxide was measured precisely before and after the VHP® process, and the results are shown in Table 10. In summary, the results indicated that there were no statistical differences in weight change among the boards and aviation wires that were exposed to VHP® and those that were not exposed.

Chemical Analysis of Aviation Wires

Chemical analyses on the printed circuit boards and aviation wire insulation (MIL227597/34-20) were performed by Raman spectroscopy. This process used an Invia Confocal Raman Microscope with a 514.5 nm wavelength and 1 mW laser excitation source. The Spectra were recorded using a 50x objective lens which generated a 1 µm laser spot. Additional examination of the surface composition of copper layer on the test boards was accomplished using X-ray photoelectron spectroscopy (XPS) and Auger electron spectroscopy. The glass transition temperature of the wire insulation layer was measured by differential scanning calorimetry (DSC). Complete chemical analyses of the epoxy resin on the FR4 board and the acrylic coating using Raman Spectroscopy can be found in the previous report of effects of hydrogen peroxide on common aviation structural materials (1).

Figure 29 shows the results from Auger electron spectroscopy on the copper layer of the print circuit boards. The major peaks include Cu, O, and C. No significant chemical changes were found even after 25 VHP® cycles. XPS results (Figure 30) on the copper layer revealed small surface changes on the sample exposed to 25 VHP® cycles. The binding energy between $2p_{1/2}$ and $2p_{3/2}$ increased slightly from 19.4 eV to 20.3 eV. This increase is an indication of an increase in the presence of CuO. Upon closer inspection of the $2p_{3/2}$ peak, one can see that only CuO feather is present (see the 25 VHP® cycle data in the magnified image in Figure 30). Table 11 shows the surface elemental composition for the control and exposed specimens. The percentage of oxygen atoms increased

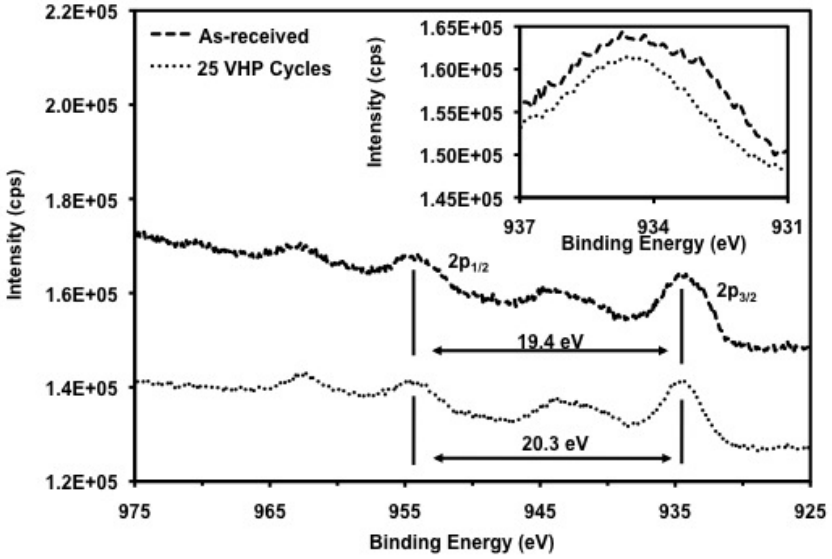

Figure 30: XPS of the Copper Layer on the Print Circuit Board. Insert Shows the 2p3/2 Peak

from 27 % for the control sample to 41 % for the exposed sample, and the presence of Cl and Sn was due to surface contamination.

Results from the Raman spectroscopy of aviation wire insulation (MIL227597/34-20) are shown in Figure 31. Extraction of the characteristic bands from the insulation material was difficult, because the surface of the insulation layer contains chemicals that raise the fluorescence noise (curving background). To accomplish the extraction, data were collected from eight tests and normalized using a fifth-order polynomial. Peaks at 1445 cm^{-1} and 2970 cm^{-1} were assigned to CH_2 and CH vibration, respectively (7, 8). Additionally, the CF vibration band was observed at 840 cm^{-1} as shown in the magnified image in Figure 31. These characteristic bands did not show any shift at their corresponding wave numbers, and no extra peaks were found after 10 VHP® cycles. DSC results (shown in Figure 32) indicated that the glass transition temperature of the wire insulation remained unchanged for specimens exposed to 10 VHP® cycles. Having the same glass transition temperature in the two samples means that there were no bond changes (chemically) that allowed the polymer chains to start moving/vibrating at the transition between the glassy state and the rubbery state.

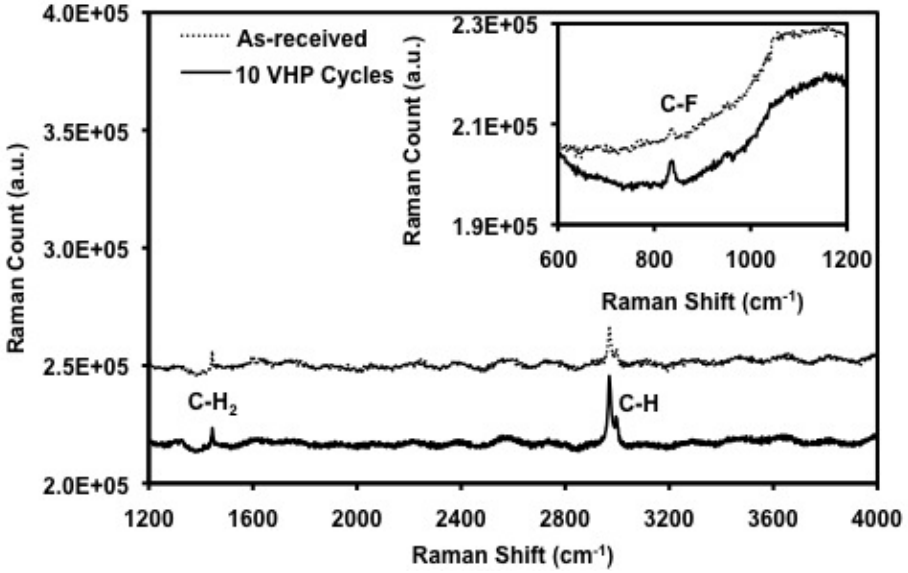

Figure 31: Raman Spectra of the Insulation Layer on the Aviation Wire

Table 11: Surface Elemental Composition of the Print Circuit Board by XPS

	Surface Elemental Composition (atom %)					
Specimen	Cu	O	C	N	Cl	Sn
Control	14	27	52	1	5	1
25 VHP®	11	41	45	0	0	3

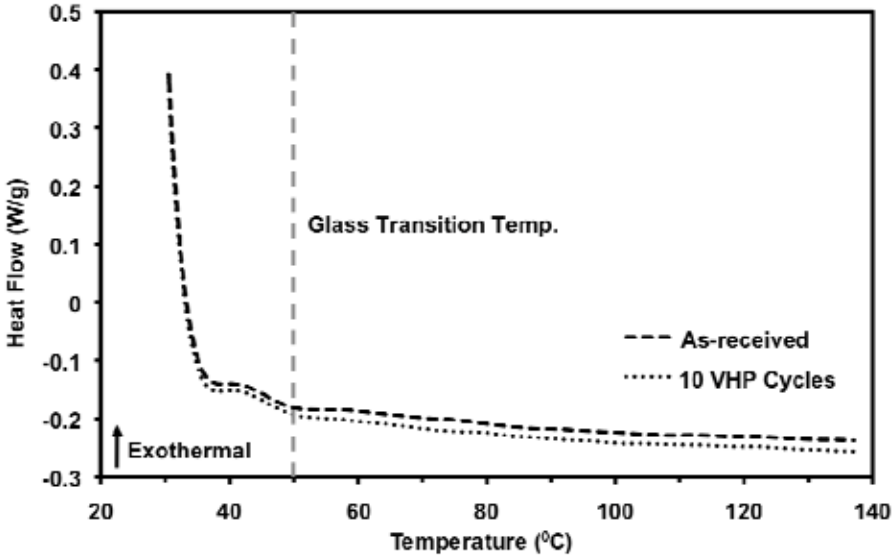

Figure 32: DSC Diagram of the Insulation Layer on the Aviation Wire

CONCLUSIONS

The above results have lead to the development of several important conclusions. First, VHP® exposure had no affect on the circuit boards. The discoloration of the copper boards would have occurred even in ambient environmental conditions. Furthermore, resistance and impedance readings were recorded at different frequencies. The results showed no statistical differences between the boards exposed to VHP® and those not exposed to VHP®. Also, for the active circuit boards, the input and output signals for the same board before and after VHP® exposure showed only minor differences. These variations could easily be the result of circuit noise. As for the aviation wires, the data indicate that the fail time of exposed wires was noticeably shorter (on average). However, the voltage used for the tests was determined to be above any realistic level. As of this writing, additional tests are being conducted at more realistic voltage levels. Finally, for the weight change and chemical analysis, the results indicated that there were no statistical differences in weight change and no degradation/oxidation chemically between the boards and wires that were exposed to VHP® and those that were not exposed.

REFERENCES

1. S.F. Chou, M.H. Sk, N.I. Sofyan, R.A. Overfelt, W.F. Gale, H.S. Gale, C.G. Shannon, J.W. Fergus, and J. Watson, "Evaluation of the Effects of Hydrogen Peroxide on Common Aviation Structural Materials," FAA Technical Report DOT/FAA/AM-09/23, 2009, Washington, DC: Office of Aerospace Medicine.
2. W.F. Gale, H.S. Gale, and J. Watson, "Field Evaluation of Whole Airliner Decontamination Technologies for a Narrow-Body Aircraft," FAA Technical Report DOT/FAA/AM-08, 2008, Washington, DC: Office of Aerospace Medicine.
3. R.M. Shaftstall, R.P. Garner, J. Bishop, L. Cameron-Landis, D.L. Eddington, G. Hau, S. Spera, T. Mielnik, and J.A. Thomas, "Vaporized Hydrogen Peroxide (VHP®) Decontamination of a Section of a Boeing 747 Cabin," FAA Technical Report DOT/FAA/AM-06/10, 2006, Washington, DC: Office of Aerospace Medicine.
4. W.F. Gale, H.S. Gale, and J. Watson, "Field Evaluation of Whole Airliner Decontamination Technologies— Wide-Body Aircraft With Dual-Use Application for Railcars," FAA Technical Report DOT/FAA/AM-08/4, 2008, Washington, DC: Office of Aerospace Medicine.

5. W.D. Callister, Jr. and D.G. Rethwisch, Fundamentals of Materials Science and Engineering, 3rd Ed., Indianapolis, IN: John Wiley, 2007, pp. 695.

6. Bare Board Cleanliness by Surface Insulation Resistance, IPC-TM-650 Test Methods Manual, Association Connecting Electronics Industries, January 2004.

7. L.F. Santos, R. Wolthuis, S. Koljenovic, R..M. Almeida, and G.J. Puppels, "Fiber-Optic Probes for in Vivo Raman Spectroscopy in the High Wavenumber Region," Analytical Chemistry, 2005, 77(20), pp. 6747-52.

8. S. Phongtamrug, K Tashiro, A. Funaki, K. Arai, and S. Aida, "Structural Study of a Series of Ethylene-Tetrafluoroethylene Copolymers with Various Ethylene Contents, Part 1: Structure at Room Temperature Investigated for Uniaxially-Oriented Samples by an Organized Combination of 2D-WAXD/SAXS and IR/Raman Spectra," Polymer, 2008, 49, pp. 561-9.